ADVANCED MATERIALS

tained at approximately 80 °C by a heating tape and were subsequently calcined at 400 °C for 4 h to remove the surfactant [16]. Mesoporous silica microparticles thus obtained were modified by surface grafting according to the procedure described by Huang and Wirth [22] adapted to *N*-isopropylacrylamide (NIPAAm). Hydroxyl groups were created on the silica surface by treatment with concentrated HNO_3 for 4 h and subsequent washing with ultra-pure (> 18 MΩ resistance) water and then drying at 110 °C for 2 h under an N_2 stream. These particles (0.5 g) were then added to a reactor containing 0.5 mL of the initiator, 1-(trichlorosilyl)-2-(*m*/*p*-(chloromethyl) phenyl)ethane (Gelest), and 50 mL of anhydrous toluene. The reaction was carried out at room temperature for 12 h. The silica particles were then washed with toluene, methanol, and acetone and dried at 110 °C for 2 h. Atom transfer radical polymerization (ATRP) was performed on the initiator-derivatized particles. 0.2 g of silica particles were combined with 0.107 g CuCl, 0.5 g of bipyridine, and 3 g of NIPAAm (Aldrich) in 30 mL of dimethyl formamide. The reaction flask was deoxygenated with N_2 for 40 min and then sealed under N_2. The reaction took place at 130 °C for 40 h with stirring. The grafted particles were then washed with methanol and water and dried at 70 °C under a stream of N_2.

The particles were characterized by SEM (Hitachi S-800) and X-ray diffraction (Siemens D5000, Cu Kα radiation $\lambda = 1.5418$ Å). Particle sizes were measured from the SEM images. Surface area and pore size distribution studies were carried out using nitrogen adsorption and desorption at 77 K using a Micromeritics ASAP 2000 porosimeter. Sample preparation for cross-sectional transmission electron microscopy (JEOL 2010, 200 KV) required the particles to be embedded in an epoxy and then cross-sectioned using a Sorvall MT-5000 Ultra Microtome machine.

Polymer-modified particles (1.0 mg) were added to 1.0 mL of 0.035 mM fluorescein in Tris buffer (0.05 M, pH 7.4) and were incubated at either 25 or 50 °C for 2 h. The samples were then cooled down to room temperature (~25°C), and equilibrated at this temperature for at least 40 min. The particles were then washed three times in fresh Tris buffer. Flow cytometry recorded the dye remaining in the particles at both 50 °C and 25 °C. The uptake of dye was also measured, using flow cytometry, at various temperatures to examine the temperature response of the grafted polymer.

Bead suspensions were analyzed by flow cytometry using a Becton-Dickinson FACScan flow cytometer (Sunnyvale, CA) interfaced to a Power PC Macintosh using the Cell Quest software package. The FACScan is equipped with a 15 mW air-cooled argon ion laser. The laser output wavelength is fixed at 488 nm. Experimental details of these analyses have been described elsewhere [23,24].

For confocal microscopy, 5.0 mg of polymer grafted particles were incubated in 0.4 mL of an aqueous solution containing 0.5 mM of rhodamine 6G (Molecular Probes) at either 25 or 50 °C overnight. The samples were then cooled to room temperature (~25°C), and equilibrated at this temperature for at least 40 min. The particles were washed two times with water at room temperature. The dye remaining in the particles was observed at 50 °C or 25 °C using a confocal laser scanning microscope at regular intervals. Microscopy was performed on a Zeiss Axiovert microscope using an LSM 510 (Carl Zeiss) scan head. Simultaneous DIC imaging was performed using the scan head and LSM software and a Plan Neo Fluor 40X/1.3 NA oil immersion lens. A He–Ne laser (543 nm) was used to excite fluorescence. Samples were heated by placing a suspension of particles on a slide supported on a heating stage constructed from an aluminum block and a self-adhesive heating element. The temperature of the sample was probed using a thermocouple.

Received: March 26, 2003
Final version: May 2, 2003

[1] C. Kresge, M. Leonowicz, W. Roth, C. Vartuli, J. Beck, *Nature* **1992**, *359*, 710.
[2] J. Y. Ying, C. P. Mehnert, M. S. Wong, *Angew. Chem. Int. Ed*. **1999**, *38*, 56.
[3] T. E. Patten, K. Matyjaszewski, *Acc. Chem. Res.* **1999**, *32*, 895.
[4] H. G. Schild, *Prog. Polym. Sci*. **1992**, *17*, 163.
[5] D. M. Jones, J. R. Smith, W. T. S. Huck, C. Alexander, *Adv. Mater.* **2002**, *14*, 1130.
[6] T. Ito, T. Hioki, T. Yamaguchi, T. Shinbo, S. Nakao, S. Kimura, *J. Am. Chem. Soc*. **2002**, *124*, 7840.
[7] G. V. R. Rao, M. E. Krug, S. Balamurugan, H. Xu, Q. Xu, G. P. Lopez, *Chem. Mater*. **2002**, *14*, 5075.
[8] I. Y. Galev, B. Mattiasson, *Trends Biotechnol.* **1999**, *17*, 335.
[9] A. Chilkoti, M. R. Dreher, D. E. Meyer, D. Raucher, *Adv. Drug Delivery Rev.* **2002**, *54*, 613.
[10] G. W. Webber, E. J. Wanless, V. Butun, S. P. Armes, S. Biggs, *Nano Lett.* **2002**, *2*, 1307.
[11] N. K. Mal, M. Fujiwara, Y. Tanaka, *Nature* **2003**, *421*, 350.
[12] J. Lahann, S. Mitragotri, T. Tran, H. Kaido, J. Sundaram, I. S. Choi, S. Hoffer, G. A. Somorjai, R. Langer, *Science* **2003**, *299*, 371.
[13] A. Kikuchi, T. Okano, *Adv. Drug Delivery Rev.* **2002**, *54*, 53.
[14] A. S. Hoffman, *Clin. Chem.* **2000**, *46*, 1478.
[15] S. Balamurugan, S. Mendez, S. S. Balamurugan, M. J. O'Brien, G. P. Lopez, *Langmuir* **2003**, *19*, 2545.
[16] G. V. R. Rao, G. P. Lopez, J. Bravo, A. K. Datye, H. Xu, T. L. Ward, *Adv. Mater*. **2002**, *14*, 1301.
[17] Y. Lu, H. Fan, A. Stump, T. L. Ward, T. Reiker, C. J. Brinker, *Nature* **1999**, *398*, 223.
[18] A. Sellinger, P. M. Weiss, A. Nguyen, Y. Lu, R. A. Assink, W. Gong, C. J. Brinker, *Nature* **1998**, *394*, 256.
[19] H. Y. Fan, Y. F. Lu, A. Stump, S. T. Reed, T. Baer, R. Schunk, V. Perez Luna, G. P. Lopez, C. J. Brinker, *Nature* **2000**, *405*, 56.
[20] D. Bontempo, N. Tirrelli, K. Feldman, G. Masci, V. Crescenzi, J. A. Hubbell, *Adv. Mater.* **2002**, *14*, 1239.
[21] M. Kamigaito, T. Ando, M. Sawamoto, *Chem. Rev*. **2001**, *101*, 3689.
[22] X. Huang, M. J. Wirth, *Anal. Chem*. **1997**, *69*, 4577.
[23] T. Buranda, G. P. Lopez, J. Keij, R. Harris, L. A. Sklar, *Cytometry* **1999**, *37*, 21.
[24] T. Buranda, G. Jones, J. Nolan, J. Keiji, G. P. Lopez, L. A. Sklar, *J. Phys. Chem. B* **1999**, *103*, 3399.
[25] E. B. Zhulina, O. V. Borisov, V. A. Pryamitsyn, T. M. Birshtein, *Macromolecules* **1991**, *24*, 140.
[26] J. Crank, *The Mathematics of Diffusion*, 2nd ed., Oxford University Press, New York **1975**, pp. 90–91.
[27] G. V. R. Rao, G. P. Lopez, *Adv. Mater.* **2000**, *12*, 1692.
[28] G. V. R. Rao, S. Balamurugan, D. E. Meyer, A. Chilkoti, G. P. Lopez, *Langmuir* **2002**, *18*, 1819.

Self-Assembly of Mesostructured Conjugated Poly(2,5-thienylene ethynylene)/Silica Nanocomposites**

By *Byron McCaughey*, *Chris Costello*, *Donghai Wang*, *J. Eric Hampsey*, *Zhenzhong Yang*, *Chaojun Li*, *C. Jeffrey Brinker*, and *Yunfeng Lu**

Nanocomposites, consisting of intricate combinations of organic, inorganic, and/or metallic phases arranged on the nanometer scale, have attracted a great deal of attention due to their unique ability to combine and tailor overall physical properties and due to synergy, interfacial, and confinement effects between the constituent phases.[1] Nanocomposites that contain conjugated polymers such as poly(phenylene vinylene),[2] polyaniline,[3,4] polydiacetylene,[5] poly(phenylene butadiynylene),[6] polythiophene, polypyrrole, and polyacetylene[7,8] confined within a silica matrix have shown enhanced conductivity, mechanical strength, processability, environmen-

[*] Prof. Y. Lu, B. McCaughey, D. Wang, J. E. Hampsey
Chemical Engineering Department, Tulane University
300 Lindy Boggs, New Orleans, LA 70118 (USA)
E-mail: ylu@tulane.edu
Dr. C. Costello, Prof. C. Li
Chemistry Department, Tulane University
2015 Percival Stern, New Orleans, LA 70118 (USA)
Dr. Z. Yang
State Key Laboratory of Polymer Physics and Chemistry
The Chinese Academy of Sciences
Beijing 100080 (P.R. China)
Prof. C. J. Brinker
Advanced Materials Laboratories, University of New Mexico
1001 University Boulevard SE, Suite 100, Albuquerque, NM 87106 (USA)

[**] The authors thank Dr. J. Tang, Dr. W. Zhou, Windong Chen at University of New Orleans Tulane University for assistance with XRD and TEM. This research was supported by the NSF/EPA joint program under grant NSF-DMR-0124765 and Sandia National Laboratories.

 © 2003 WILEY-VCH Verlag GmbH & Co. KGaA, Weinheim **DOI:** 10.1002/adma.200304931

tal stability, and other unique properties that allow for potential use in light emitting diodes,[9] information storage devices, optical signal processors, battery substitutes, and solar energy converters.[10] Areneethynylene conjugated polymers such as poly(2,5-thienylene ethynylene) (PTE) are particularly interesting because they have exhibited high quantum yields,[11] lower bandgaps than benzene analogs,[12] and stability to air and moisture.[13]

Conjugated polymer/ceramic nanocomposites are typically synthesized via a multiple-step synthesis process involving the formation of mesoporous material and subsequent monomer infiltration and polymerization;[2–4,6–8] however, polymerizations of conjugated polymers like polyacetylene often require strict synthesis conditions.[10] Recently, we developed a robust, one-pot polymer synthesis procedure to prepare PTE via the palladium-catalyzed polymerization of aryl diodides with acetylene gas in aqueous media.[14] The use of water as the reacting medium enables the use of the surfactant self-assembly synthesis route[15] to produce mesostructured conjugated polymers or composites.

This research utilizes the evaporation-induced co-assembly of silica, surfactant, and organic components in a mixed alcohol/water medium to form mesostructured PTE/silica nanocomposites.[16] Beginning with a homogenous solution of soluble silica, hydrophobic catalytic species, 2,5-diiodothiophene polymer precursors, and surfactant in ethanol/water solvent; solvent evaporation during the coating process enriches nonvolatile components and induces their co-assembly into liquid crystalline mesophases. Polymerization of silica during the coating process freezes the mesophases and spatially organizes the catalyst and polymer precursor into hexagonal, cubic, or lamellar silica mesostructures.[17,18] The subsequent Sonogashira coupling reaction of acetylene with the incorporated 2,5-diiodothiophene and Pd catalyst[19] forms a PTE/silica nanocomposite that retains the original liquid-crystalline mesostructure. As opposed to the commonly utilized multistep infiltration techniques, this one-step approach provides a simple route to spin-coat, dip-coat, or inkjet print thin films and patterned arrays of mechanically stable conjugated polymer/silica nanocomposites.[17,18,20]

X-ray diffraction (XRD) performed on a series of spin-coated samples outlined the three successive stages of nanocomposite formation. Figure 1 shows XRD spectra of mesostructured films A) without the incorporation of monomer or catalyst, B) with the incorporation of monomer and catalyst but prior to polymerization, and C) after polymerization. Diffraction peaks at 45, 49, and 53 Å *d*-spacing in scan (A) are respectively attributed to cubic mesophase [211], [210], and [200] orientations.[21] As shown in the inset to Figure 1, these diffraction peaks shift to higher *d*-spacing due to the incorporation of monomer/catalyst (scan B) and to the further incorporation and reaction of acetylene gas that forms the PTE (scan C) within the hydrophobic core of the liquid-crystalline mesophase.

Figure 2 shows representative transmission electron microscopy (TEM) images of the polymer/silica nanocomposites.

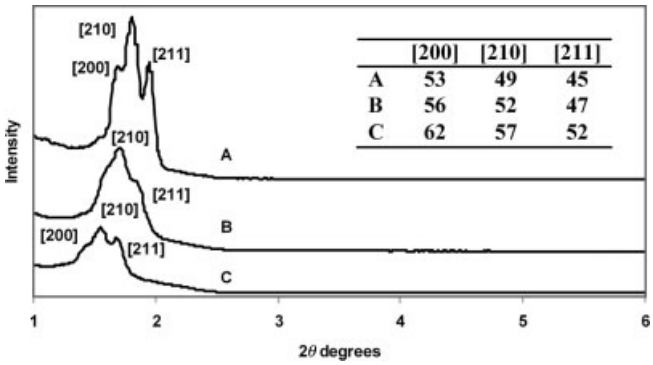

	[200]	[210]	[211]
A	53	49	45
B	56	52	47
C	62	57	52

Fig. 1. XRD of mesostructured silica/surfactant thin films: A) without monomer or catalyst; B) with catalyst and monomer incorporation but prior to polymerization; C) after polymerization yielding a PTE/silica nanocomposite. Inset table shows peak positions in angstroms.

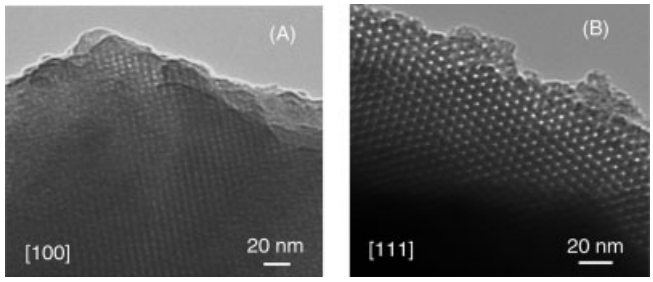

Fig. 2. TEM images of PTE/silica nanocomposite with cubic mesostructure viewed from A) [100] orientation and B) [111] orientation.

The highly ordered nanocomposite shows a center-to-center spacing of A) 58 Å and B) 64 Å, which may be attributed to the [100] and [111] orientations of a cubic mesophase, respectively. Shrinkage of the samples in the TEM chamber may cause a decrease in these *d*-spacing values in comparison to the XRD results shown in Figure 1C. Energy dispersive spectroscopy (EDS) elemental analysis identified silicon, oxygen, carbon, and sulfur as expected for the PTE/silica nanocomposite. After silica removal, the porous nanostructure of the poly(2,5-thienylene ethynylene) was observed by TEM; however, this structure was very sensitive to the electron beam and no images could be recorded.

Polymer formation was further verified by UV-vis and FTIR spectroscopy. Figure 3 shows the UV-vis spectra of thin films A) without catalyst or monomer, B) with catalyst and monomer but prior to polymerization, and C) after polymerization. A shoulder peak at 365 nm in (B) indicates the presence of Pd catalyst complex prior to polymerization. Polymerization initiated by exposing the catalyst–monomer complex to acetylene gas results in a more intense absorbance especially above 300 nm (C), which is similar to those of areneethynylene polymers that show an absorbance between 350 and 600 nm.[22] FTIR spectroscopy on PTE polymer after silica and surfactant removal shows strong thiophene stretching bands at 1602 and 1436 cm^{-1}; out of plane thiophene C–H bending bands at 1097 and 1004 cm^{-1}; and low intensity ethynylene vibration around 2260 cm^{-1} due to the symmetry of the ethynylene substitutes.

 © 2003 WILEY-VCH Verlag GmbH & Co. KGaA, Weinheim

ADVANCED MATERIALS

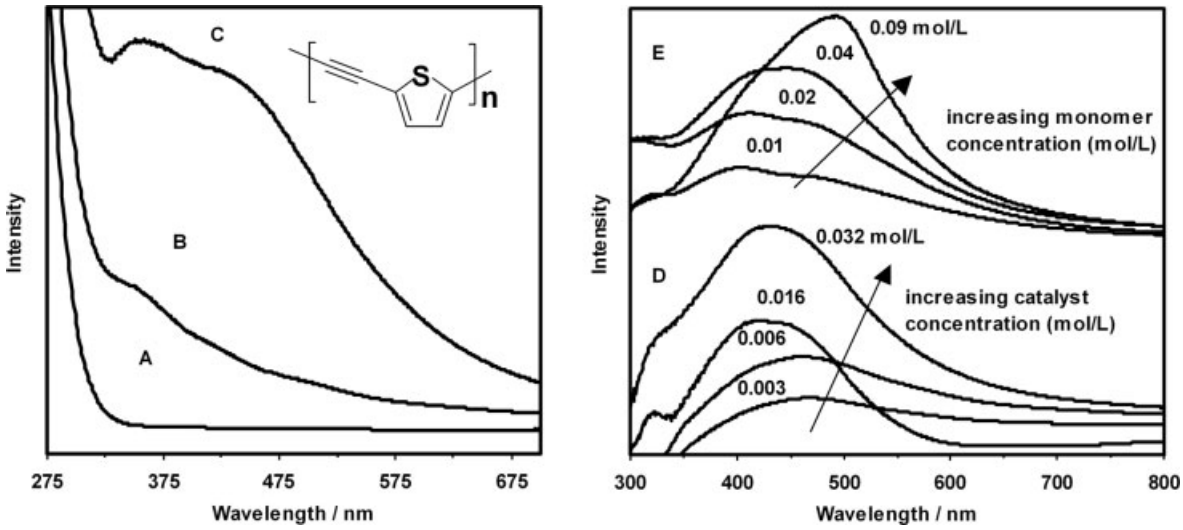

Fig. 3. UV-vis spectra of thin films: A) without catalyst or monomer; B) with catalyst and monomer but prior to polymerization; C) after polymerization showing the presence of Pd catalyst complex and poly(2,5-thiophene ethynylene); D) prepared using different concentrations of catalyst and E) monomer (spectra after catalyst peak subtraction). Expected PTE structure shown in inset.

PTE chain rigidity[22] results in low solubility,[23] and a low degree of polymerization.[24] Direct molecular weight determination is difficult. In this research, we attempted to study the degree of polymerization using UV-vis spectroscopy. Figure 3D,E shows UV-vis spectra of the nanocomposites prepared with different concentrations of catalyst (D) and monomer (E). Increasing the monomer concentration from 0.01 to 0.09 mol L^{-1} shifts the absorption band from 406 to 495 nm with an increase in absorption intensity. An increase in catalyst concentration from 0.003 to 0.032 mol L^{-1} also increases the absorption intensity but shifts the absorption from 469 to 431 nm. Oligomeric 2,5-thiophene ethynylene with 1–4 repeat units shows UV-vis peaks from 317 to 400 nm,[12] while PTE with an average molecular weight of 21 600 exhibits a UV absorbance that monotonically decreases from 200 nm to 600 nm.[13] Since polymer with longer chains may exhibit UV-vis peaks at higher wavelengths, our results indicate that the degree of polymerization increases as the monomer concentration increases or as the catalyst concentration decreases. However, the exact molecular weight of our polymer is still uncertain and further experimentation is needed.

Thermal stability of the nanocomposites was studied by simultaneous differential thermal analysis/thermogravimetric analysis (DTA/TGA). Figure 4 shows the DTA/TGA curves of A) pure mesostructured polymer after surfactant and silica removal and B) as-reacted polymer/silica/surfactant nanocomposites. The small, sharp endothermic peak around 70 °C on curve B is due to the removal of residual solvent. The weight losses of approximately 15 % (A) and 35 % (B) around 350 °C are caused by the decomposition of short chain hydrocarbons such as oligomeric products, surfactant, and PPh_3. The exothermic peaks at 226 °C may have been the evidence of thermal cross-linking or polymer chain realignment.[25] In both samples, polymer decomposition is indicated by a broad endothermic peak accompanied by a gradual weight loss

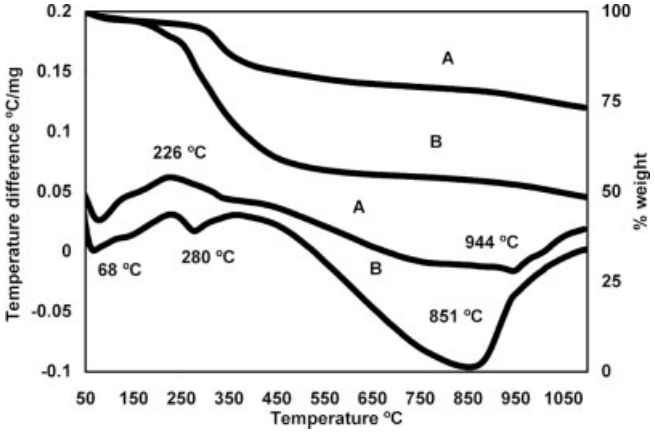

Fig. 4. Simultaneous DTA (bottom two lines)/TGA (top two lines) of A) pure poly(2,5-thienylene ethynylene) after silica and surfactant removal and B) as-reacted polymer/silica/surfactant nanocomposite.

above 600 °C. For the composite (B), the remaining weight of 40–50 % at 1100 °C corresponds to the initial carbon and silica contained in the composite. On the other hand, the pure polymer (A) retains close to 75 % of its weight as residual carbon at 1100 °C, which is also consistent with its initial carbon composition (~ 68 %).

We have demonstrated the formation of conjugated PTE/silica nanocomposites by a novel sol–gel self-assembly and an air- and water-insensitive organometallic-catalyzed polymerization method. The robustness of this synthesis is further demonstrated by the ability of the oligomeric PTE thin films to continuously react with acetylene gas that results in darkened films with increased UV-vis absorptions. This approach provides a unique and ready route to synthesize nanostructured conjugated polymer and composites. Future work will focus on the studies of their mechanical, electrical, electroluminescent, and other properties of these nanocomposites with various mesostructures and compositions.

 © 2003 WILEY-VCH Verlag GmbH & Co. KGaA, Weinheim

Experimental

Tetraethoxysilane (TEOS), nitric acid, surfactant, and 2,5-diiodothiophene were mixed in tetrahydrofuran (THF) at room temperature for half an hour to form a precursor solution. The catalytic complex was formed by reacting palladium acetate, cuprous iodide, and triphenylphosphine (PPh_3) in THF. A typical synthesis utilizes a molar ratio of reactants of THF/HNO_3/TEOS/Brij-58/PPh_3/CuI/Pd$(OAc)_2$/2,5-diiodothiophene of 6.2:0.356:0.937:0.1:0.04:0.014:0.017:0.1, where Brij-58 is a non-ionic surfactant $CH_3(CH_2)_{15}(OCH_2CH_2)_{20}OH$. Films were prepared by either spin-coating the mixture of the catalytic complex and precursor solutions onto glass slides using a Specialty Coating Systems P-6000 spin-coater or allowing them to evaporate in a petri dish to form xerogels. The thin films were exposed to acetylene gas and triethylamine vapor at room temperature and 50 psi pressure for up to 3 days to polymerize the incorporated monomer. Pure conjugated PTE was obtained by washing with dilute HF to remove the silica and by ethanol extraction to remove the surfactant. The PTE was washed with ethanol to remove the unbound catalyst and partially dissolved in chloroform to achieve oligomeric PTE solutions that were subsequently coated on glass slides to form red oligomeric PTE films. The oligomeric PTE films were exposed to acetylene gas and the continuous reactions of acetylene with the active complex attached to the oligomers resulted in darkened films with increased UV-vis absorptions.

The nanocomposites were characterized by transmission electron microscope (TEM, JEOL 2010, operated at 200 kV), X-ray diffraction (XRD, Phillips Xpert X-ray diffractometer using Cu Kα radiation at $\lambda = 0.1542$ nm), UV-vis spectroscopy (Beckman DU460B UV-vis), Fourier transform infrared spectroscopy (FTIR, Thermo Nicolet Nexus 670 spectrophotometer with a Smart MIRacle horizontal attenuated total reflectance Ge crystal accessory), and by differential thermal analysis and thermogravimetric analysis (DTA/TGA, 2960 Simultaneous DTA–TGA by TA Instruments) operated at 10 °C min^{-1} from 30 to 1200 °C with argon sweep gas.

Received: January 28, 2003
Final version: April 10, 2003

[1] H. Eckert, M. Ward, *Chem. Mater.* **2001**, *13*, 3059.
[2] T.-Q. Nguyen, J. Wu, S. H. Tolbert, B. J. Schwartz, *Adv. Mater.* **2001**, *13*, 609.
[3] C.-G. Wu, T. Bein, *Science* **1994**, *266*, 1013.
[4] C.-G. Wu, T. Bein, *Chem. Mater.* **1994**, *6*, 1109.
[5] Y. Lu, Y. Yang, A. Sellinger, M. Lu, J. Huang, H. Fan, R. Haddad, G. Lopez, A. R. Burns, D. Y. Sasaki, J. Shelnutt, C. J. Brinker, *Nature* **2001**, *410*, 913.
[6] V. S.-Y. Lin, D. R. Radu, M.-K. Han, W. Deng, S. Kuroki, B. H. Shanks, M. Pruski, *J. Am. Chem. Soc.* **2002**, *124*, 9040.
[7] C. R. Martin, *Science* **1994**, *266*, 1961.
[8] D. J. Cardin, S. P. Constantine, A. Gilbert, A. K. Lay, M. Alvaro, M. S. Galletero, H. Garcia, F. Marquez, *J. Am. Chem. Soc.* **2001**, *123*, 3141.
[9] D. D. C. Bradley, *Adv. Mater.* **1992**, *4*, 756.
[10] W. J. Feast, J. Tsibouklis, K. L. Pouwer, L. Groenendaal, E. W. Meijer, *Polymer* **1996**, *37*, 5017.
[11] A. P. Davey, S. Elliott, O. O'Connor, W. Blau, *J. Chem. Soc., Chem. Commun.* **1995**, 1433.
[12] G. V. Tormos, P. N. Nugara, M. V. Lakshmikantham, M. P. Cava, *Synth. Met.* **1993**, *53*, 271.
[13] Y. S. Gal, B. Jung, S. K. Choi, *J. Appl. Polym. Sci.* **1991**, *42*, 1793.
[14] C.-J. Li, W. T. Slaven, V. T. John, S. Banerjee, *Chem. Commun* **1997**, *16*, 1569.
[15] J. Israelachvili, in *Intermolecular and Surface Forces*, 2nd ed., Academic Press Inc., San Diego, CA **1992**.
[16] A. Sellinger, P. M. Weiss, A. Nguyen, Y. Lu, R. A. Assink, C. J. Brinker, *Mater. Res. Soc. Symp. Proc.* **1998**, *519*, 95.
[17] A. Sellinger, P. M. Weiss, N. Anh, Y. Lu, R. A. Assink, W. Gong, C. J. Brinker, *Nature* **1998**, *394*, 256.
[18] C. J. Brinker, Y. Lu, A. Sellinger, H. Fan, *Adv. Mater.* **1999**, *11*, 579.
[19] R. H. Crabtree, in *The Organometallic Chemistry of the Transition Metals*, 3rd ed., Wiley-Interscience, New York **2001**.
[20] Y. Lu, G. Cao, R. P. Kale, S. Prabakar, G. P. Lopez, C. J. Brinker, *Chem. Mater.* **1999**, *11*, 1223.
[21] Q. Huo, D. I. Margolese, G. D. Stucky, *Chem. Mater.* **1996**, *8*, 1147.
[22] R. Giesa, *J. Macromol. Sci., Rev. Macromol. Chem. Phys.* **1996**, *C36*, 631.
[23] G. Shi, S. Jin, G. Xue, C. Li, *Science* **1995**, *267*, 994.
[24] W. T. I. V. Slaven, C.-J. Li, Y.-P. Chen, V. T. John, S. H. Rachakonda, *J. Macromol. Sci., Pure Appl. Chem.* **1999**, *A36*, 971.
[25] D. R. Rutherford, *Ph.D. Thesis*, Colorado State University, Fort Collins, CO **1989**, pp. 170.

Enhancement of Photocatalytic and Electrochromic Properties of Electrochemically Fabricated Mesoporous WO_3 Thin Films**

By *Sung-Hyeon Baeck*, *Kyoung-Shin Choi*, *Thomas F. Jaramillo*, *Galen D. Stucky*, and *Eric W. McFarland**

Tungsten oxide (WO_3) is an indirect bandgap semiconductor with interesting photoconductive behavior that has potential applications as a low cost material for solar energy devices.[1,2] Because of its distinct photochromic response and intercalation properties (H^+, Li^+, Na^+, and K^+),[3] it has also found use in electrochromic devices and chemical sensors. For the hydrogen cations, the electrochromic process of tungsten oxide has been explained on the basis of the double intercalation of a proton and an electron to form a colored tungsten bronze. WO_3 has been prepared by physical and chemical methods including sputtering and vacuum evaporation.[4] Electrochemical synthesis has been accomplished by stabilizing tungsten ions in sulfuric acid[5] or as a peroxo complex.[6,7] Because of the versatility of tungsten oxide in photo-electrochemical processes, the formation of high surface area, mesoporous tungsten oxide has also been of interest.[8–15] Synthesis of porous oxides has followed early work on catalytic functional materials such as MCM-41 using surfactants and block copolymers as templates.[16–21] Cheng et al.[9] reported enhanced electrochromic properties of sol–gel synthesized mesoporous tungsten oxide; however, the material did not exhibit long-range order of the pores. In general, synthesis of well-ordered tungsten or molybdenum oxides has been limited by the formation of Keggin ions and difficulties in promoting their three-dimensional condensation to give stable mesoporous structures.

We have recently described an electrochemical strategy for the production of thin nanostructured films by utilizing potential-controlled self-assembly of surfactant–inorganic aggregates at solid–liquid interfaces.[22] This approach manipulates surfactant–inorganic assemblies only in the thin interfacial region by electrochemically controlling surface interactions, which allows for the formation of nanostructured films from dilute surfactant solutions. After deposition, surfactants can

[*] Prof. E. W. McFarland, Dr. S.-H. Baeck, T. F. Jaramillo
Department of Chemical Engineering, University of California
Santa Barbara, CA 93106-5080 (USA)
E-mail: mcfar@engineering.ucsb.edu
Prof. G. D. Stucky
Department of Chemistry and Biochemistry, University of California
Santa Barbara, CA 93106-5080 (USA)
K.-S. Choi
Department of Chemistry, Purdue University
West Lafayette, IN 47907-2084 (USA)

[**] Major funding was provided by the Hydrogen Program of the Department of Energy (DOE, Grant # DER-FC36-01G011092). Partial funding and facilities were provided by the NSF-MRSEC funded Materials Research Laboratory (Award # DMR96-32716). Partial funding (GDS) was also supported by the National Science Foundation (NSF Grant # DMR02-33728).

 DOI: 10.1002/adma.200304669 © 2003 WILEY-VCH Verlag GmbH & Co. KGaA, Weinheim